Angular distributions of the atomic scandium $3d$ and $4s$ photoelectrons in the region of the $3p \rightarrow 3d$ giant resonance

S. B. Whitfield,[1,*] T. Myers,[1] M. Bjelland,[2] R. Wehlitz,[3] J. Jiménez-Mier,[4] P. Olalde-Velasco,[4] and M. O. Krause[5]

[1]*Department of Physics and Astronomy, University of Wisconsin-Eau Claire, Eau Claire, Wisconsin 54702*
[2]*Department of Chemistry, University of Wisconsin-Eau Claire, Eau Claire, Wisconsin 54702*
[3]*Synchrotron Radiation Center, University of Wisconsin, Stoughton, Wisconsin 53589*
[4]*Instituto de Ciencias Nucleares, UNAM, 04510 Mexico City, Mexico*
[5]*Department of Physics, University of Central Florida, Orlando, Florida 32816*

A determination of the angular distribution parameter β of the $3d$ and $4s$ main lines of atomic scandium in the resonance region of the $3p \rightarrow nd, ms$ excitations has been carried out using electron spectrometry in conjunction with monochromatized synchrotron radiation. These measurements reveal strong variations of β throughout the entire resonance region, highlighting the complicated nature of the ionization process for this first and seemingly simple $3d$ transition metal. The β values of the photoelectrons resulting in $4s$ subshell ionization deviate significantly from 2.0 in qualitative, but not quantitative, agreement with recent many-body perturbation-theory calculations.

The experimental determination of the angular distribution parameter β of photoelectrons provides a crucial test for theoretical methods beyond that provided by partial cross sections alone. This is because β depends on the relative phases of the outgoing partial waves in addition to the transition matrix elements. Open-shell atoms add yet another layer of complexity, because there are typically three different terms that characterize the final state of the ion plus photoelectron; while for closed shell atoms there is only one, a ^1P term (we restrict our discussion to dipole transitions only). Even for the photoemission of a single partial wave, the presence of these additional terms can lead to interesting effects in the photoionization process, which cannot occur in closed-shell atoms. A prime example is the s-subshell photoionization where even in the absence of relativistic effects β of the photoelectrons can deviate significantly from 2.0 [1–5]. For s-subshells of closed-shell atoms in the absence of relativistic effects, β is always 2.0. Despite such intrinsically interesting effects that can arise in the photoionization of open-shell atoms, there are still relatively few studies of them as compared to what has been done on closed-shell atoms, chiefly the rare gases, and far fewer involving angular distribution measurements. This can largely be attributed to the difficulty in producing a usable atomic beam of open-shell atoms.

Atomic Sc with a lone $3d$ electron, $[\text{Ar}]3d4s^2(^2D_{3/2})$, is in principle the simplest open-shell atom to have a partially filled d subshell. This makes detailed studies of atomic Sc particularly attractive both theoretically and experimentally. Following our recent experiments of the partial cross sections of the $3d$ and $4s$ main and satellite lines of atomic Sc in the region of the $3p \rightarrow 3d$ giant resonance [6], we report here β measurements of the $3d$ and $4s$ main lines in the same photon energy region. These measurements were partly motivated by recent many-body perturbation theory (MBPT) calculations of the $4s$ angular distributions in the $3p \rightarrow 3d$ resonance region [7].

The experiment was conducted at the University of Wisconsin Synchrotron Radiation Center on the plane grating monochromator with an undulator photon source [8]. Energy selected photons from the monochromator are directed through a glass capillary into a resistively heated Ta crucible, where Sc atoms are produced by evaporation of the solid. The crucible used in this experiment differs from that used previously [6], in that it has *two* slits in it to allow the photoelectrons to pass directly from the oven into two analyzers that are mounted perpendicular to the photon beam at $0°$ and $90°$ with respect to the polarization vector of the synchrotron radiation. For additional details of the experimental setup see Refs. [6,9]. At typical oven temperatures of 1170 °C, thermal excitation produces 56% of the target atoms in the $^2D_{5/2}$ excited state and 44% in the ground state.

The angular distribution parameter β can be determined from the ratio R of the measured intensities at $0°$ and $90°$ if the degree of linear polarization, p, of the incident photon beam is known [3]. We measured p to be 0.993(5). R was corrected for possible differences in the source volume as seen by the two analyzers as well as for differences in the detection efficiency of the two analyzers as determined from Ne $2s$ and $2p$ calibration spectra. Once β has been obtained, then the relative partial cross section σ can be derived from either the $0°$ or the $90°$ spectrum. Spectra were recorded primarily in the constant ionic state (CIS) mode in which a photoelectron line is scanned synchronously with the photon energy. The resolution of a CIS spectrum depends solely on the bandpass of the monochromator. The resolution of the electron spectrometer only plays a role insofar as it must be capable of isolating single final states of the ion. In this measurement we used the same slit settings as previously [6], where a bandpass of 20(3) meV at 47.7 eV was determined.

As in our earlier partial cross section measurements [6], five different CIS spectra were recorded for each main line at a given angle to cover the photon energy range from 29.0 to 40.4 eV. The step size was 10 meV. A detailed explanation of the analysis procedures involving the raw CIS scans is given in Ref. [6].

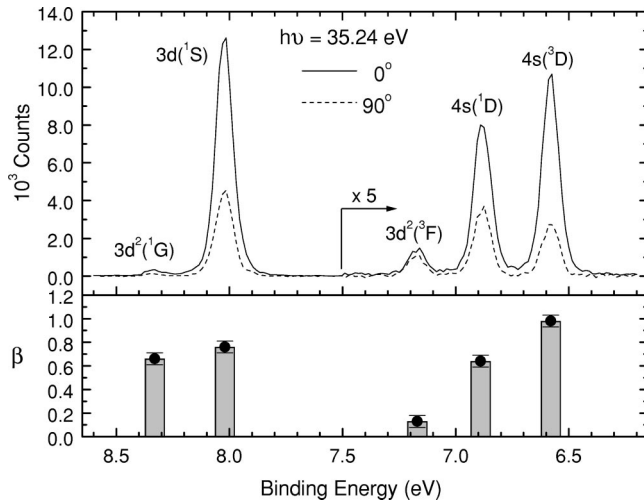*Electronic address: whitfisb@uwec.edu

FIG. 1. Top panel, high-resolution photoelectron spectrum of the $3d$ and $4s$ main lines and nearby satellite lines (FWHM is 84 meV) recorded at at the maximum of the $3p \rightarrow 3d$ giant resonance. The step size is 15 meV. Bottom panel, β values of the photoelectron lines.

A high-resolution photoelectron spectrum (PES) of the atomic Sc main lines and nearby satellites recorded by the 0° and 90° analyzers at $h\nu = 35.24(2)$ eV is shown in Fig. 1. This photon energy corresponds to the maximum value of the cross section of the $3d(^1S)$ main line in the region of the $3p \rightarrow 3d$ transitions. As in our earlier paper [6], we will refer to the main lines according to the subshell of the electron removed in the photoionization process, and *not* by the ionic state left behind: thus, the $3d(^1S)$ designation refers to the $[\mathrm{Ar}]4s^2(^1S)$ final-ionic state, and $4s(^{3,1}D)$ to the $[\mathrm{Ar}]3d4s(^{3,1}D)$ final-ionic states. The binding energy scale was established by setting the $3d(^1S)$ photoline to 8.015 eV as derived from optical data [10]. The lower panel shows the β values for all lines in the spectrum. Both the 0° and 90° spectra have been corrected for background, source volume asymmetries, and analyzer detection efficiencies. Clearly evident for both $4s$ lines is a strong deviation from $\beta = 2.0$. In the absence of relativistic effects such a deviation from $\beta = 2.0$ is not possible for s-subshell photoelectrons of closed-shell atoms, even in the presence of autoionizing resonances. The significant difference in the β value of the two $4s$ lines can be attributed to the difference in their spin multiplicities. At this energy we obtain the following β values for the main lines: $\beta_{3d(^1S)} = 0.76(5)$, $\beta_{4s(^1D)} = 0.63(5)$, $\beta_{4s(^3D)} = 0.98(5)$.

The dynamical behavior of β through a series of resonances is revealed in greatest detail by employing the CIS technique. Panels (a) and (b) of Figs. 2–4 show the CIS spectra of the $3d$ and $4s$ main lines recorded at 0° and 90°, respectively, while panel (c) shows the resulting β curve. Panel (d) shows our derived partial cross section, σ, using the 0° spectrum and the β curve. A comparison of these derived partial cross sections with those measured directly [6] shows excellent overall agreement, which gives us added confidence in the accuracy of our β curves. The positions of two of the five $3p$ thresholds, the ^3P and the ^3F [6], are
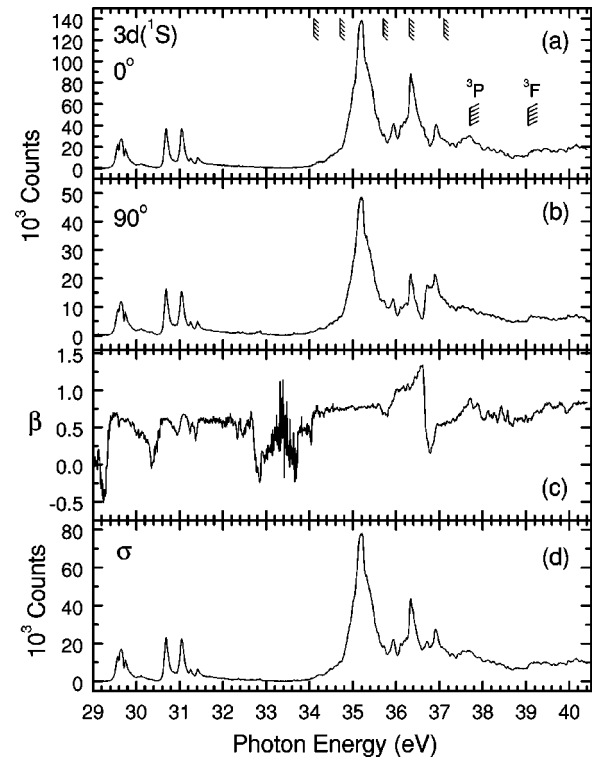

FIG. 2. The $3d(^1S)$ main line. (a) CIS 0° spectrum; (b) CIS 90° spectrum; (c) β; (d) derived partial CIS σ spectrum. See text for additional details.

indicated in panel (a) (the other three thresholds lie above the photon region shown here). Also shown are five of the ionization thresholds associated with $3p$ ionization of a secondary configuration $[\mathrm{Ar}]3d^24s(^2D)$ that mixes with the primary $[\mathrm{Ar}]3d4s^2(^2D)$ ground-state configuration [6,11]. All values of R used to derive the β curves for the main lines were scaled such that they would yield the same β at $h\nu = 35.24(2)$ eV as obtained from our PES results. Thus, systematic errors associated with these PES results could shift the curves as a whole. However, the relative error within the β curve is given by the statistical scatter of the data points. These spectra are displayed without any correction to the photon energy scale, which is estimated to have about a 20 meV accuracy. Absolute peak positions of those resonances lying between 29.0 and 32.0 eV can be found in Ref. [6].

The $3d$ β curve, Fig. 2, is essentially flat with frequent excursions. The very noisy region between about 33.2 and 34 eV is due to the very low statistics in both the 0° and 90° spectra due to a minimum in the $3d$ cross section at this energy. Perhaps surprisingly, there is almost no variation of β across the large resonance feature at $h\nu = 35.24$ eV. The largest excursion occurs at about 36.7 eV and is due to a resonance that becomes quite prominent in the 90° spectrum, but is hardly seen in the 0° spectrum. The next largest excursion occurs on the lower-energy flank of the resonance structure that peaks at about 29.6 eV. Very recent calculations [12] of the total cross section of atomic Sc in this photon energy region have identified this resonance as being composed primarily of the $^2D_{3/2} \rightarrow 3p^54s^23d^2(^1G)^2F_{5/2}$ and the $^2D_{5/2} \rightarrow 3p^54s^23d^2(^1G)^2F_{7/2}$ transition, indicating the im-
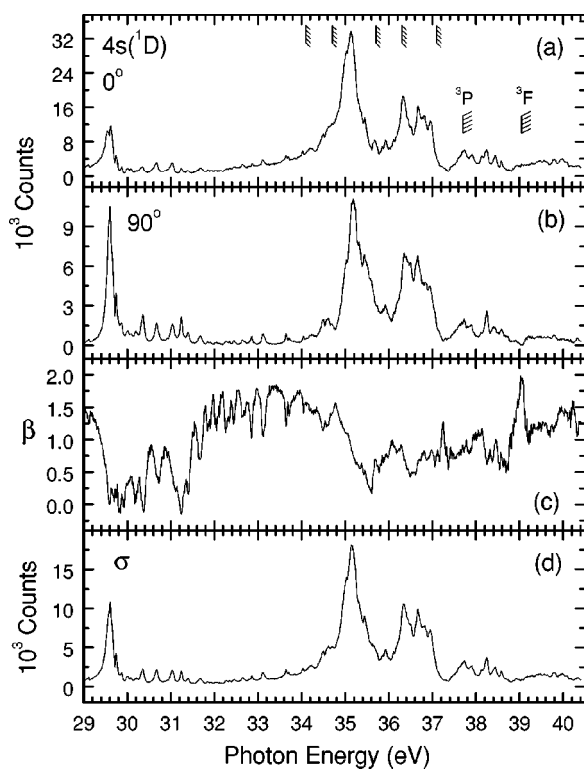
FIG. 3. The $4s(^1D)$ main line. Otherwise as for Fig. 2.
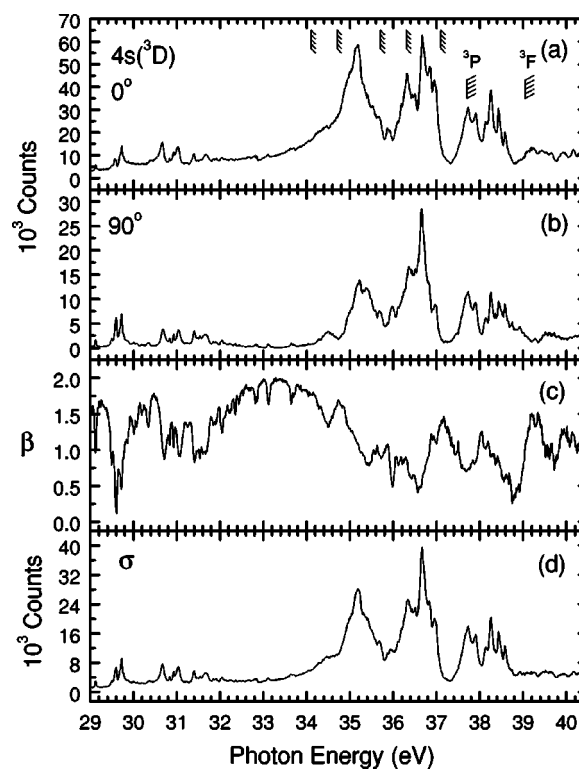
FIG. 4. The $4s(^3D)$ main line. Otherwise as for Fig. 2.

portance of accounting for photoionization from the excited state of the neutral. This feature has a strongly negative β value at its minimum, in contrast to the other transitions that are generally positive. The same sort of windowlike excursions also appear on the low-energy flanks of the "rabbit ears" at 30.7 and 31.1 eV.

The two $4s$ lines, Figs. 3 and 4, show dramatic deviations from $\beta=2.0$ throughout the entire resonance region, highlighting the open-shell character of this atom. Both lines show qualitatively similar behavior, which is, not surprisingly, quite distinct from what is observed for the $3d$ line. Detailed differences between the two $4s$ β curves are due to the different spin multiplicities of the two lines. In both cases β dips substantially from a value of about 1.5 at 29 eV to almost zero near the center of the feature at 29.6 eV. While the $4s(^1D)$ line continues to show strong modulations over the next 1.5 eV, the $4s(^3D)$ line essentially returns to its initial value of 1.5 before another strong set of modulations begin which are associated with the resonances beginning at 30.7 eV and continuing to about 31.8 eV. For both $4s$ lines, and in particular the $4s(^1D)$ line, there are substantial excursions in β from about 31.6 eV to about 34.0 eV. As can be seen from the CIS spectra, these are due to the very weak resonances that are scattered throughout this photon energy region. Only a few of these resonances are visible in the $3d$ CIS spectra where only the feature just above 32.8 eV exhibits a large excursion in the $3d$ β curve. It is worth noting that the $4s(^3D)$ line very nearly approaches $\beta=2.0$ at about 33.4 eV. While the $4s(^1D)$ line also reaches a local maximum at this energy, it is closer to 1.8 than 2.0. In contrast to the $3d$ line there is a significant change in β for both $4s$ lines across

the large resonance located at 35.2 eV. The rather strong excursion in β that is seen in both $4s$ lines near 39.0 eV, particularly the $4s(^1D)$ line, may be due to the presence of the $3p(^3F)$ ionization threshold.

Figure 5 shows a comparison of our measured β values to those calculated in Ref. [7]. A convolution procedure [13] using a 20-meV Gaussian profile has been applied to the theoretical curves so that a direct comparison with experiment can be made. As can be seen, there is not particularly good agreement between theory and experiment. This is not surprising since these calculations are based on the same MBPT formalism in LS coupling that was used to obtain the partial cross sections of the $3d$ and $4s$ main lines [14], which were shown earlier [6] to be at variance with experiment. Nevertheless, a detailed comparison does provide some useful information. For the experimental $4s(^1D)$ line from 29.0 to about 31.4 eV there is partial qualitative agreement with theory from 29.0 eV to about 32.5 eV. Similarly, for the experimental $4s(^3D)$ line from 29.0 to about 30.5 eV there is again partial qualitative agreement with theory from 29.0 to 32.5 eV. This suggests that while the absolute magnitudes of the transition matrix elements for these excitations are greatly over estimated [6,14], their relative magnitudes and phases give β values that are in better agreement with experiment. It is also worth noting that the overall magnitude of the excursions from $\beta=2.0$ is very consistent between experiment and theory (most are between $\beta=2.0$ and 0), particularly for the $4s(^3D)$ line. Above the large resonance at 35.2 eV in the experimental CIS spectra, Rydberg excitations of the $3p$ electrons become energetically possible. As can be seen from the CIS spectra and the β curves, there is
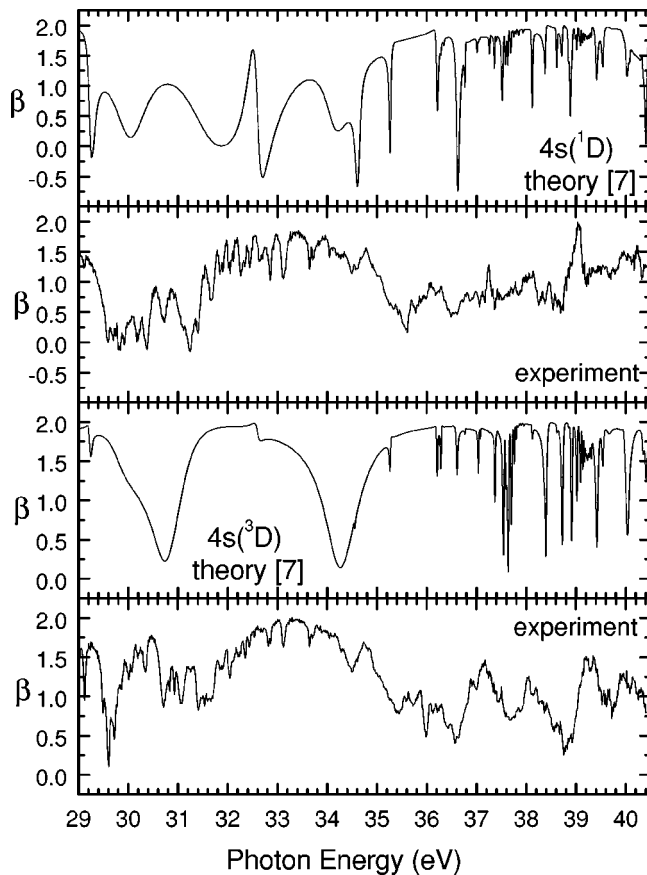
FIG. 5. Comparison of β between theory and experiment. Top two panels, $4s(^1D)$; bottom two panels, $4s(^3D)$.

little evidence for any sharp well resolved Rydberg structure in this region, whereas theory predicts many sharp and well isolated lines. This lack of Rydberg structure in the experimental spectra is not due to our bandpass, but is partly the result of the decay of these excitations into continua associated with the thresholds of the $[Ne]3s^23p^53d^24s$ ionic con-

figuration [6,11]. This additional decay pathway causes a substantial broadening of the Rydberg lines [15,16]. This broadening, in addition to the close spacing of the Rydberg excitations, leads to the large broad structures observed in the spectra. A lack of the inclusion of these additional decay pathways is a primary reason the MBPT theory [7,14] predicts a very sharp, well isolated Rydberg structure. In the more recent calculations of Martins [12] the $[Ne]3s^23p^53d^24s$ final-ionic states, among many others, are included explicitly in the calculation of the photoabsorption cross section and a much better agreement with experiment [6] is obtained.

Finally, one of the interesting predictions made in Ref. [7] is the effect of the interchannel coupling on the $4s$ β values outside the resonance region investigated here. We looked for such effects; unfortunately, the cross section of the $4s$ photoelectrons is so small that it was not possible to obtain any off-resonance $4s$ β values.

In conclusion, we have presented a detailed examination of the angular distributions of the main lines of atomic Sc in the region of the $3p\rightarrow3d$ giant resonance. Our results, particularly for the $4s$ lines, show strong variations of β throughout the entire photon energy region examined. Differences between the two $4s$ lines arise from their different spin multiplicities. A comparison of our CIS data with the only existing angular distribution calculations reveals major discrepancies. It is hoped that these results will spur theorists to make improved calculations for this seemingly simple $3d$ transition metal.

[1] A.F. Starace, R.H. Rast, and S.T. Manson, Phys. Rev. Lett. **38**, 1522 (1977).

[2] S.T. Manson and A.F. Starace, Rev. Mod. Phys. **54**, 389 (1982).

[3] S.B. Whitfield, K. Kehoe, M.O. Krause, and C.D. Caldwell, Phys. Rev. Lett. **84**, 4818 (2000).

[4] H. P. Saha, Phys. Rev. A **66**, 010702(R) (2002).

[5] Z. Felfli, N. C. Deb, D. S. F. Crothers, and A. Z. Msezane J. Phys. B. **35**, 419 (2002).

[6] S.B. Whitfield, K. Kehoe, R. Wehlitz, M.O. Krause, and C.D. Caldwell, Phys. Rev. A **64**, 022701 (2001).

[7] Z. Altun and S.T. Manson, Phys. Rev. A **61**, 030702(R) (2000).

[8] R. Reininger, S.L. Crossley, M.A. Lagergren, M.C. Severson, and R.W.C. Hansen, Nucl. Instrum. Methods Phys. Res. A **347**, 304 (1994).

[9] M.O. Krause, T.A. Carlson, and A. Fahlman, Phys. Rev. A **30**, 1316 (1984).

[10] J. Sugar and C. Corliss, J. Phys. Chem. Ref. Data Suppl., **14**, 1 (1985).

[11] H. E. Wetzel, Dissertation, University of Hamburg, 1987, unpublished.

[12] M. Martins, J. Phys. B **35**, L223 (2002).

[13] J.G. Childers, D.B. Thompson, and N.L.S. Martin, Phys. Rev. A **64**, 062703 (2001)

[14] Z. Altun and S.T. Manson, Europhys. Lett. **33**, 17 (1996); Phys. Rev. A **59**, 3576 (1999).

[15] C.D. Caldwell, M.O. Krause, R.D. Cowan, A. Menzel, S.B. Whitfield, S. Hallman, S.P. Frigo, and M.C. Severson, Phys. Rev. A **59**, R926 (1999).

[16] M. Martins, J. Phys. B **34**, 1321 (2001).